Letter Report

RELATIVE BIOLOGICAL EFFECTIVENESS OF LOW-ENERGY ELECTRONS AND PHOTONS

Prepared by

Michael Bellamy and Keith Eckerman
Environmental Sciences Division
Oak Ridge National Laboratory
Oak Ridge, Tennessee 37831

October 20, 2013

Work sponsored by:

Office of Radiation and Indoor Air
U. S. Environmental Protection Agency (EPA).

OAK RIDGE NATIONAL LABORATORY

MANAGED BY UT-BATTELLE FOR
THE DEPARTMENT OF ENERGY

PREFACE

A draft of the letter report was submitted for review to Drs. Wesley Bolch, Dudley Goodhead, and David Kocher. This report reflects the comments and suggestions offered in the review. The critical issue of the review was whether the approach adopted in the letter report was reasonable; that is, deriving RBE values for electrons and photons based on the cumulative fraction of absorbed dose below 5 keV. The approach is empirical and employs Monte Carlo simulation of individual electron tracks passing through the absorbing material. It was shown that the results are reasonably consistent with available experimental information and with the theoretical calculations of other investigators. An alternative to the 5-keV threshold was investigated in an appendix to the reviewed report but because of its weak basis it was removed from the final report as suggested in the review.

In general the reviewers found the report to be sound and clear although areas for clarification were noted and address in the final report. For example, it was suggested to clearly note the adoption of 1 MeV electrons as the reference radiation rather the more common photon reference of experimental investigations; e.g., Co-60 photons. It was also suggested that photon RBE values be evaluated under both first interaction and complete absorption considerations. Thus RBE values for photons (first interaction and complete absorption) were derived for electrons liberated by photon interactions. The RBE for Co-60 derived in this manner was found to be 1.03 (first interaction) and 1.08 (complete absorption) with their average being 1.06. For the A-bomb photon spectra at a 1500 m ground distance the average RBE is 1.01. Tritium, the only internally incorporated radionuclide for which much experimental evidence is available, was found to have an RBE be 2.05. In the application of these data in revision of Federal Guidance Report 13 the issue regarding usage of “relative biological effectiveness – RBE” versus “radiation effectiveness factor – REF” needs to be addressed.

ABSTRACT

There is growing evidence to support a relative biological effectiveness (RBE) greater that one for low-energy electrons and photons. Strong justification of an RBE greater than one for low energy electrons comes from radiobiological studies of tritium. Similarly, studies with low-energy photons have indicated an elevated response relative to reference radiations of higher energy. In the field of radiation protection, photons and electrons have been assigned a radiation weighting factor (w_R) of one. While this value may be appropriate for radiation protection calculations, it is important in risk considerations to consider the potentially elevated effectiveness of these radiations in efforts to improve the quality of the radiogenic risk estimates. Low-energy electron and photon radiations produce dense ionization clusters which lead to RBE values greater than those of high energy gamma rays. For tritium, RBE values between 2 and 3 are implied by a number of experimental studies. Other radiation sources with similar energy emissions may also exhibit an elevated RBE. In this work, RBE values are derived for electron and photon emissions based on the fractional deposition of absorbed dose for electrons of energies less than a few keV. Using this empirical model, RBE values for monoenergetic electrons, monoenergetic photons, and machine-generated x-rays were derived. In addition, nuclide-specific RBE values were calculated for the radionuclides of ICRP Publication 107 for which neither alpha decay or spontaneous fission is indicated as a mode of decay.

INTRODUCTION

Federal Guidance Report No. 13 (FGR 13), issued by the Environmental Protection Agency (EPA 1999a), tabulates radionuclide-specific risk coefficients for radiogenic cancer due to chronic intake or external exposure to radionuclides based on risk expression models set forth in a report entitled *Estimating Radiogenic Cancer Risks* (EPA 1994, 1999b). Recently EPA issued updated risk expression models (EPA 2011), for the most part based on the recommendations of the National Academy of Sciences report: *Health Risk from Exposure to Low Levels of Ionizing Radiation*, BEIR VII (NAS 2006). The parameters of the risk expression models are largely based on results of epidemiological studies of the Japanese atomic bomb survivors, who were exposed to a mixed photon and neutron radiation field. The calculation of the risk coefficients includes consideration of absorbed dose and modification of the risk projection model by a dose rate reduction factor (DDREF) and application of the relative biological effectiveness (RBE)[1] in the event of alpha radiations. There is now evidence that low-energy electrons and photons also are more damaging than high-energy photons, so that an RBE greater than 1.0 might be warranted in assessing cancer risk from these radiations.

For the purposes of radiation protection, the International Commission on Radiological Protection (ICRP, 2004), assigns a radiation weighting factor (w_R) of 1.0 to radiations of low linear energy transfer (LET); i.e., electrons and photons. This value is invariant with energy despite the fact that the LET of these radiations varies with energy. A constant w_R is a convenient assumption within radiation protection (Dietze and Alberts 2004); however, ICRP noted in the preface to Publication 92 (ICRP, 2004) that:

> "… w_R is a quantity intended for use in radiological protection and was not developed for use in epidemiological studies or other specific investigations of human exposure. For these other studies, absorbed dose in the organs of interest and specific data related to the RBE of the radiation type in question are the most relevant quantities to use."

In Publication 103, ICRP (2007) further noted that the simplification of w_R equal 1 for all low-LET radiations is:

> "… sufficient only for the intended application of equivalent dose and effective dose, e.g., for dose limitation and assessment and control of doses in the low-dose range. In cases where individual retrospective risk assessments have to be made, more detailed information on the radiation field and appropriate RBE values may need to be considered if relevant data are available."

This letter report addresses the potential application of an energy-dependent RBE for low-LET radiations in the calculation of cancer risk coefficients.

Experimental studies with electron and photon radiations have shown an elevated low-energy RBE (Goodhead *et al*. 1981, Goodhead & Nikjoo, 1990, Hill 2004, Little & Lambert 2008, Nikjoo & Lindborg 2010). Generally, in these experiments cell populations were exposed to varying radiation doses and the resulting biological responses evaluated. A variety of cell types including human epithelial cells, human melanoma cells, mouse fibroblast cells, and yeast cells have been studied. The biological endpoints varied

[1] Kocher et al. (2005) have introduced the term radiation effectiveness factor (REF) as the quantity representing the biological effectiveness of radiations when estimating cancer risks and thus restrict the use of RBE to the results of radiobiological studies. However in this work we continue to use the term RBE as a modifier of the risk expression as in efforts to derive cancer risk coefficients. Retain the earlier use should not be a cause for confusion.

but include neoplastic transformation, cell death, micronucleus formation, carcinogenesis and chromosome aberrations. The variation in RBE with electron energy has been attributed to the pattern of energy deposition in tissue. As the electron energy is reduced, ionization and excitation interactions in tissue become more localized. This clustering of interactions leads to an increased frequency and complexity in DNA damage that may result in misrepair and initiation of mutations. Based on both experimental data and computational simulations of DNA damage, it has been suggested that mutational interactions are strongly dependent on the fraction of energy deposited by electrons at energies below about 5 keV (Nikjoo & Goodhead 1991). This is expected to be true even for higher energy electron and photon sources, as such radiations result in a sequence of interactions that generate a large number of secondary electrons and delta rays, particularly near the ends of their tracks.

Based on an analysis by Burch (1957a, 1957b), Nikjoo and Goodhead (1991) estimated that 25 to 35% of the absorbed dose from incident 100-2000 keV electrons is deposited by interactions at energies below 5 keV. For the tritium (^{3}H) beta (average energy 5.7 keV, end point energy 18.8 keV), this fraction was estimated to be about 75%. Nikjoo and Goodhead observed that an RBE for ^{3}H in the range of 2 to 3 relative to ^{60}Co gammas was consistent with the calculated relative fractions of absorbed dose deposited by electrons of energy less that 5 keV from ^{3}H and ^{60}Co, as initially indicated by Burch. Current Monte Carlo methods can provide more precise estimates of the energy deposition processes of electrons.

Electron track structure codes have been used by a number of investigators to study the spatial distribution of ionizing interactions (Turner *et al*. 1981, Moiseenko *et al*. 2000, Nikjoo *et al*. 2001, Friedland *et al*. 2008). Biological damage may be simulated by overlaying a calculated electron track onto a DNA model and quantifying the potential interactions. A breakage classification scheme for DNA is shown in Fig. 1 (Charlton & Humm 1988). In this scheme, a double strand break (DSB) is considered possible when two single strand breaks (SSB) occur on opposite DNA strands and are separated by less than 10 base-pairs. The complexity of the DNA models that follow this approach varies widely, ranging from a straight segment of the double strand DNA helix (Turner *et al*. 1981) to a full atomistic representation of the folded human chromosome (Friedland *et al*. 2008). The underlying physics and chemistry involved in generating the electron tracks also vary among these models. Some models address only physical ionization events along the track while others include pre-chemical and chemical steps representing the production of radicals and their diffusion in tissue.

The induction of biological endpoints such as carcinogenesis is likely to be a complex function of electron energy. Computer simulations indicate both increased production of simple DSBs with increasing ionization density and more complex, clustered damage involving DSBs with additional nearby strand breaks (Fig. 1) or sites of base damage (Nikjoo *et al.* 1997, 2001, 2002). For low energy electrons, roughly 20-30% of the simulated DSBs are a complex type by virtue of SSBs occurring within 10 base pairs. Misrepair of complex DSBs, as well as that of multiple, closely spaced single strand breaks (SSBs) with or without nearby base damage, may contribute substantially to radiation induced mutations. Due to gaps in our current knowledge of repair efficiencies for various types of complex damage and the relative contributions of different types of damage, the RBE for cancer induction cannot be derived from first principles even if the initial damage could be accurately estimated.

An elevated response to low LET radiation has been incorporated into the probability-of-causation calculations of the National Institute for Occupational Safety and Health (NIOSH) and the U.S. Department of Labor (DOL). These considerations are documented in reports by NIOSH (2002), the National Cancer Institute (NCI), and Centers for Disease Control and Prevention (CDC) (Land *et al*. 2003). See Kocher *et al*. (2005) for a detailed review of the relative response of electron and photon radiations of various energies.

In a report on tritium the Advisory Group on Ionizing Radiation (AGIR) to the UK Health Protection Agency concluded (HPA 2007):

> "In a wide variety of cellular and genetic studies RBE values for tritiated water have generally been observed in the range of one to two when compared with orthovoltage X-rays and in the range of two to three when compared with gamma rays. We recommend that high energy gamma rays be the preferred choice for reporting RBE values…"

The AGIR report recommends that an RBE value of 2 be adopted for estimating risk from tritiated water and that consideration (pending international consensus) be given to the use of a radiation weighting factor (w_R) of 2 for radiation protection purposes. Kocher *et al*. (2005) assigned tritium an RBE assuming a lognormal probability distribution with a geometric mean of 2.4 and geometric standard deviation of 1.4 (95% confidence interval 1.2 to 5.0).

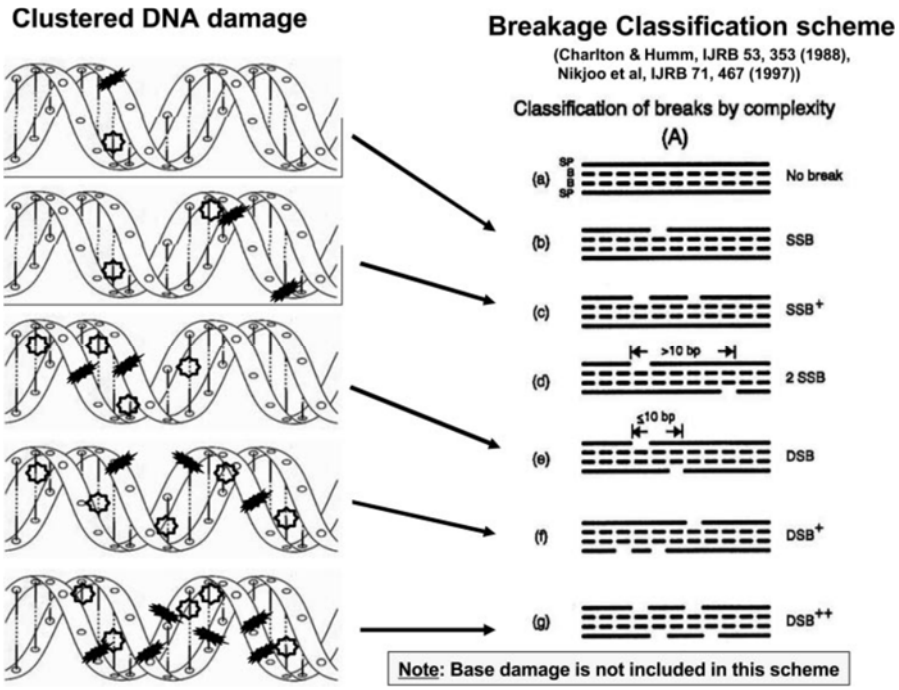

Fig. 1. Breakage classification scheme for various types of DNA damage used in computational modeling (Goodhead, 2006).

The appropriate relative biological effectiveness (RBE) for low-energy electrons and photons was identified by EPA (2011) as an issue to be resolved before updating Federal Guidance Report 13. In the present report, an electron track code is used to derive RBE values across a range of electron energies from 1 keV to 1.0 MeV following the empirical approach of Nikjoo and Goodhead (1991). As the absorbed dose from photons is due to liberated electrons, photon RBE values are derived from the electron RBEs. The reference radiation in the analysis is taken to be 1 MeV electrons, not photon radiation as used for practical reasons in experimental studies. Uncertainties in the derived RBE values arise from the computational parameters and the empirical approach itself.

METHODS

Detailed aspects of the energy deposition by electrons can be investigated in mathematical simulations of electrons passing through tissue. In this work, the NOREC code (Semenenko *et al*. 2003) is used to generate tracks of electrons of initial energies ranging from 1 keV to 1 MeV. NOREC, the New Oak Ridge Electron transport Code, is an interaction-by-interaction simulator based on the original Oak Ridge Electron transport Code (Turner *et al.* 1988). The code provides information on the spatial location of ionization and excitation interactions defining the track, along with the transferred energy. An example of a NOREC generated electron track is shown in Fig. 2. Benchmark studies of NOREC with other Monte Carlo codes have shown general agreement across most electron initial energies (Cho *et al.* 2007, Dingfelder *et al*. 2008). Detailed cross section data are available for electron interactions in liquid water, which serves as an acceptable surrogate for tissue.

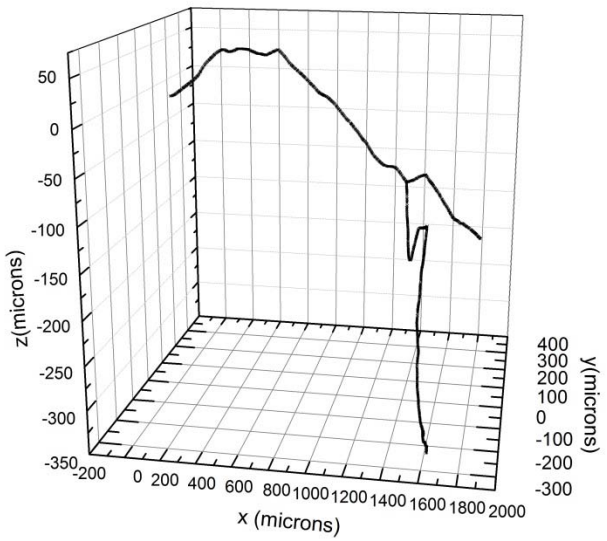

Fig. 2. The 3-D track of a 100 keV electron generated by NOREC featuring a single prominent secondary electron. The electron track starts at the origin in top left.

Electron tracks were generated by NOREC for monoenergetic electrons of initial energy E_0 ranging from 1 keV to 1 MeV. The fraction of absorbed dose deposited by interactions involving electrons of energies less than E, $F(E, E_0)$, was compiled. Secondary-electrons formed with energies less than 100 eV were treated as deposition interactions of the parent track and not as separate tracks. In essence, $F(E, E_0)$ represents the fraction of absorbed dose of an electron of initial energy E_0 deposited by interactions entered into by primary and secondary electrons of energies less than E.

Dense ionization clusters associated with low-energy electron tracks are thought to play an important role in biological damage. Michael and O'Neill (2000) described these clusters as 'a sting in the tail of electron tracks' based on studies of SSB and DSB yields in DNA after exposure to monoenergetic photons and electrons (Folkard *et al.* 1993, Boudaiffa *et al.* 2000). In addition to low-energy electrons and photons inducing a greater SSB and DSB yield, they also tend to produce more complex damage than their high-energy counterparts (Goodhead 2006). These studies highlight the increased ability of low-energy electron and photons to produce a biological effect relative to high-energy photons and suggest that the 'sting of the tail' results in an elevated RBE for these radiations.

The relative biological effectiveness of an electron of initial energy E_0, RBE(E_0), is taken to be:

$$\mathrm{RBE}(E_0) = \frac{F(E_C, E_0)}{F(E_C, E_R)} \tag{1}$$

where the numerator is the cumulative absorbed dose distribution for the radiation of interest (energy E_0) and the denominator is the corresponding distribution for the reference radiation of energy E_R. In this study, the reference radiation is taken to be electrons of energy 1 MeV.[2] The cumulative fractions of dose for the reference radiation deposited by electrons below cutoff energies E_C of 1.5, 2, 3, 4, 5, and 6 keV are listed in Table 1 and shown graphically in Fig. 3. If the initial electron energy E_0 is less the the energy cutoff E_C, then the numerator of Eqn 1 is one and the RBE is the reciprocal of $F(E_C, E_R)$.

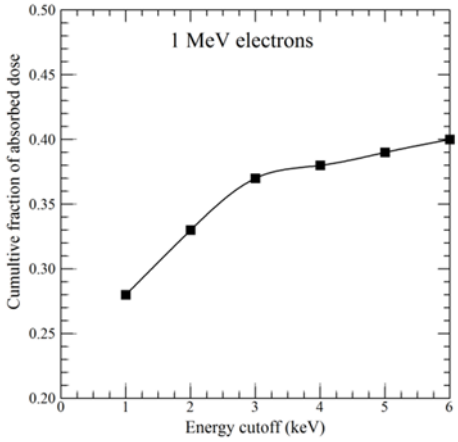

Fig. 3. Cumulative fraction of absorbed dose deposited by electrons below a specified energy for the reference radiation (1 MeV electron). Note that 30 to 40% of dose for the reference electron radiation is deposited by low-energy electrons.

Table 1. Cumulative fractions of the reference radiation, 1 MeV electron, dose due to interactions at energies below the cutoff energy, E_C.

E_C (keV)	Dose fraction
1.0	0.28
2.0	0.33
3.0	0.37
4.0	0.38
5.0	0.39
6.0	0.40

[2] Values of the RBE obtained experimentally depend on the reference radiation chosen. Generally, low-LET photon radiation is taken as the reference, although no specific energy has been agreed upon for this purpose. Experimental RBE values using either high energy x-rays (above 200 kV), ^{137}Cs or ^{60}Co gamma radiations are more relevant to assessment of radiogenic cancer.

RESULTS

Electron RBE values

Fractional cumulative absorbed dose distributions were compiled from the NOREC simulation of monoenergetic electrons ranging in energy from 0.001 to 1.0 MeV. The simulations were carried out for a total emission of 1 GeV for each monoenergetic electron; i.e, the number of simulations ranged from 10^6 at 1 keV to 10^3 at 1 MeV. The resultant cumulative absorbed dose distributions at several electron energies are shown in Fig. 4. As seen in Fig. 4, a significant fraction of the absorbed dose is deposited by low-energy secondary electrons, and the fraction increases with decreasing initial electron energy. Analysis reveals that low-energy interactions account for nearly 40% of the absorbed dose when tissue is irradiated by 1 MeV electrons. The cumulative dose curves produced by NOREC are consistent with those obtained by Nikjoo and Goodhead (1991) using MOCA8b (Paretzke 1988).

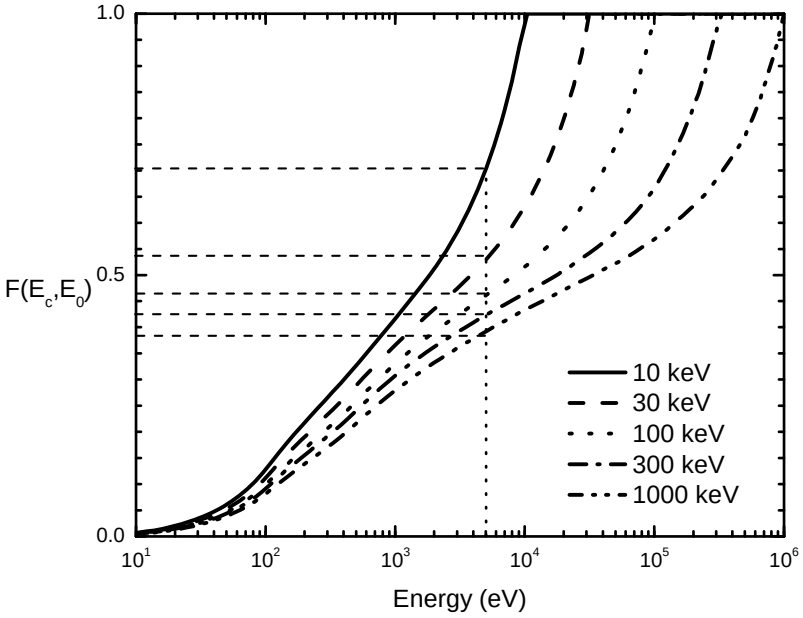

Fig. 4. Average local energy deposition by five monoenergetic electrons during passage through the absorbing medium. The data show the cumulative fraction of absorbed dose deposited by primary and secondary electrons as a function of electron kinetic energy. The fractional contribution to absorbed dose by interactions entered into at energies below a cutoff of 5 keV is projected by the horizontal lines on the y-axis.

The RBE values for monoenergetic electrons based on Eqn 1, assuming 1 MeV electrons as the reference radiation, are listed in Table 2 for energy cutoff values, E_C, ranging from 1.5 keV to 6 keV. For monoenergetic electrons of energy above 0.8 MeV the RBE values are unity for all energy cutoffs. The values gradually increase with decreasing initial electron energy and approach a maximum value at the cutoff energy. The maximum values are 3.09, 3.01, 2.72, 2.66, 2.53, and 2.44 at energy cutoffs of 1.5, 2, 3, 4, 5 and 6 keV, respectively. As shown in Fig. 5, the data of Table 2 are consistent with experimental results suggesting that low energy electrons have an elevated biological effectiveness (Hill 2004, Nijkoo 2010). The dashed lines in Fig. 5 correspond to the RBE values assigned by Kocher *et al*. (2005); i.e., a median value of 2.4 (95 % confidence interval of 1.1 to 6.1) for electrons of energies less than 15 keV and a single value of 1.0 at higher energies. This assignment was largely based on the data for low energy photons.

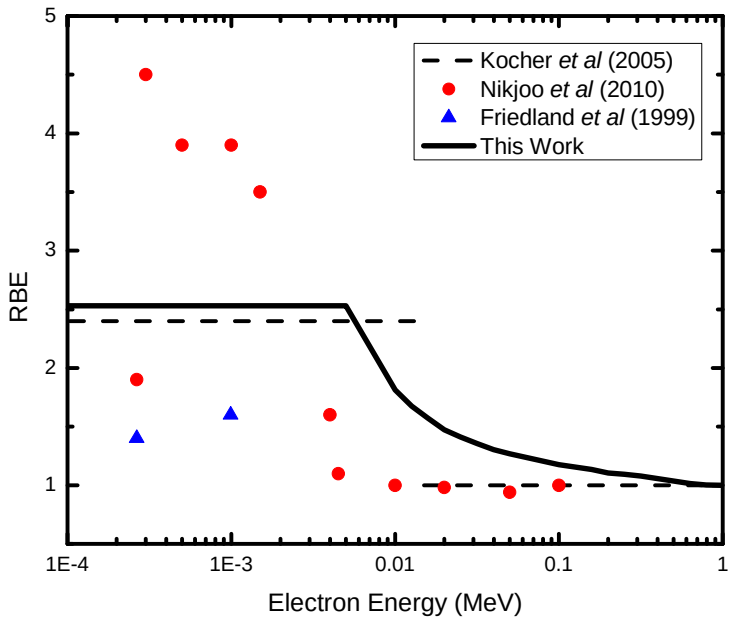

Fig. 5. Electron RBE as function of energy and values reported in various studies. The reference radiation is 1 MeV electrons and energy cutoff of 5 keV. The data points in the figure are from Friedland *et al*. (1999) and Nikjoo *et al.* (2010). The dashed line represents the recommendations of Kocher *et al*. (2005).

The RBE of tritium and other selected pure beta emitting radionuclides addressed in Table 3 are obtained by folding their beta spectra (ICRP 2008) over the electron RBE values as

$$RBE = \frac{\int_0^\infty S(E)\, E\, RBE(E)\, dE}{\int_0^\infty S(E)\, E\, dE} \qquad (2)$$

where $S(E)$ is the beta spectrum and RBE(E) is the RBE as a function of electron energy as tabulated in Table 2. The RBE values for the beta emitters of Table 3 vary little with the assumed energy cutoff values. For example, the RBEs for tritium (^{3}H) and carbon-14 (^{14}C), both common low-energy beta emitters, range from 1.7 to 2.1 and 1.2 to 1.3, respectively, depending on the choice of energy cutoff. An RBE of 2.0 for the tritium is consistent with an energy cutoff of 5 keV, and that cutoff value is adopted in our recommendations.

Photon RBE

The absorbed dose from photon radiations arises from secondary electrons liberated by photons undergoing photoelectric, Compton, and pair production interactions. RBE values for photons were derived by folding the spectrum of liberated secondary electrons over the electron RBE values in a manner similar to Eqn 2. Secondary electron spectra were generated by following the down-scattered photons in an infinite media until the incident photon energy was transferred to the media. An additional secondary electron spectrum was generated considering only the first collision (interaction) of the incident photon. The RBE values for photons ranging in energy from 0.010 to 10.0 MeV in Table 4 are based on the complete transfer of the photon energy to secondary electrons and those of Table 5 are based on the secondary electrons liberated in the first photon interaction (collision). Both tables include entries at 1.17 and 1.33 MeV, the energies of the ^{60}Co gamma rays often suggested as a reference radiation.

The dependence of the photon RBE on the electron cutoff energy is shown graphically in Fig. 6 and features a local maximum near 0.1 MeV due to the relatively high RBE values of low-energy Compton electrons formed at this energy. With decreasing photon energy below 0.1 MeV the photoelectric effect dominates the photon interactions; however, the RBE value of the photoelectrons is lower than that of Compton electrons at these energies. Below about 30 keV the RBE again increases in value with decreasing incident photon energy as photoelectric effect dominates and the photoelectrons are of low energy and high RBE value.

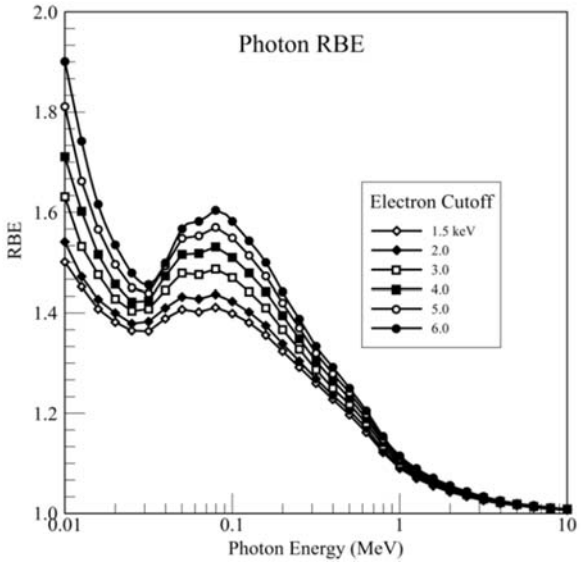

Fig. 6. RBE values for monoenergetic photons as a function of photon energy showing sensitivity to the electron energy cutoff parameter. Here all of the photon's energy is assumed to be completely absorbed in tissue and reference radiation is a 1 MeV electron**.**

A graphic comparison of photon RBE (5 keV cutoff) based on first interaction and complete absorption of the photon is shown in Fig. 7. At photon energies less than 100 keV the two derived secondary electron spectra yield similar RBE values, but above 100 keV the values are distinct. For practical purposes it is recommended that the photon RBE values be the average of the first interaction and complete absorption values as in Table 6.

The recommended photon RBE values of Table 6 are consistent with the experimental studies of Fabry and Wambersie (1985), Roos and Schmid (1988), Goggelman *et al.* (2003) and Krumey (2004) as shown in Fig. 8. Also shown in Fig. 8 are the median RBE bands assigned by Kocher *et al*. (2005) in their review of experimental data. For photon energies less than 30 keV their probability distribution has a median value of 2.4 (95% confidence interval of 1.1 to 6.1), for energies 30 to 250 keV the median of the distribution is 1.9 (95% confidence interval of 1.0 to 4.7), and above 250 keV they assign an RBE of 1.0. In a footnote, Kocher *et al*. noted that Frankenberg *et al*. (2002a, b, c) indicated that the RBE for 25-30 kVp x-rays is about 4 relative to 200 kVp x-rays and about 8 relative to ^{60}Co gamma rays. Goggelmann *et al*. (2003) report values for 29 kVp x-rays of 2 with 95% confidence interval of 1.4 to 2.6. The higher values for low-energy x-rays have been observed in *in vitro* studies. Goggelmann *et al.* suggested that infrequent change in the culture medium, as in the experiments by Frankenberg *et al.*, can cause fluctuations in the observed transformation rates. The energy dependences in the photon RBE values of Fig 8 are based on biophysical and microdosimetric principles.

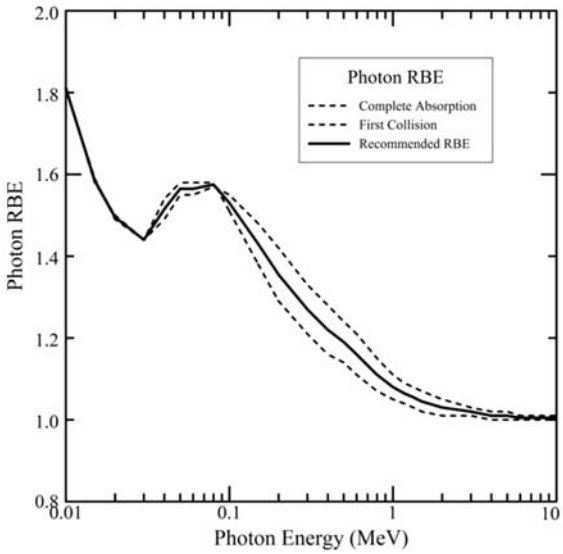

Fig. 7. A comparison of RBE values for monoenergetic photons as a function of photon energy showing the effect of assuming a first collision and complete absorption liberated electron distribution.

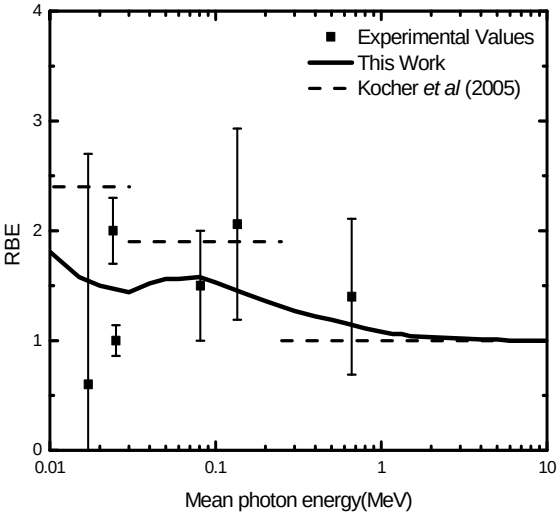

Fig. 8. Photon RBE as function of energy and values reported in various studies. The reference radiation is 1 MeV electrons. The experimental studies include Fabry and Wambersie (1985), Roos and Schmid (1988), Goggelman et al. (2003) and Krumrey (2004). The median values of the RBE probability distributions recommended by Kocher *et al*. (2005) are also shown.

Machine-generated X-rays

RBE values for machine generated x-rays were derived in a manner similar to Eqn 2 using x-ray spectra generated by the SpekCalc software package (Poludniowski *et al*. 2009). These values are listed in Table 7 for various voltages and filtration as a function of cutoff energy. The data show a moderate increase in RBE values from 120 to 20 kVp x-rays in all cases. The additional filtering of 1 mm of copper hardens the beam sufficiently to result in a slightly lower RBE value at all voltages. No appreciable difference in RBE is indicated for 20 and 250 kVp x-rays; the derived RBE is in the range 1.4-1.6, which is consistent with observations of Goggelmann *et al*. (2003).

Atomic Bomb Spectrum

Egbert *et al*. (2007) have tabulated the ground-level photon spectra at Hiroshima and Nagasaki as a function of ground distances from the hypocenter. The tissue kerma-weighted mean energy of the spectra is 3.2 and 3.3 MeV at Hiroshima and Nagasaki, respectively. The spectrum of secondary electrons liberated by the photons within the body at 1500 m ground distance was calculated using the MCNPX code (Pelowitz 2008), and the RBE was derived using the data of Table 2 for a cutoff energy of 5.0 keV. For both cities the resultant photon RBE was 1.01, slightly less than the 1.06 value for the ^{60}Co gamma rays. Based on this work ^{60}Co gamma rays are slightly more effective than Hiroshima and Nagasaki photon spectra, but not to the extent suggested by Straume (1995).

Radionuclide RBE

Radionuclide-specific RBE values were calculated for the radionuclides of ICRP Publication 107 (ICRP 2008) for which alpha emission or spontaneous fission is not indicated as a mode of decay. The calculations assume the radionuclide is uniformly distribution in the soft tissues of the adult male. The calculation of the risk coefficients in the revision of Federal Guidance Report 13 will include the age and gender specifics of the U.S. population and the distributions of the radionuclide within the tissues of the body at radiogenic risk following inhalation and ingestion intakes. For illustrative purposes, the nuclide-specific RBE for the hypothetical total-body distribution is calculated as

$$RBE = \frac{\frac{1}{M}\int_0^\infty S(E)\, RBE_E(E)\, E\, dE \;+\; \frac{1}{M}\sum_i E_i\, Y_i\, RBE_E(E_i) + \sum_i E_i\, Y_i\; SAF(E_i)\, RBE_p(E_i)}{\frac{1}{M}\int_0^\infty Y(E)\, E\, dE \;+\; \frac{1}{M}\sum_i E_i\, Y_i\, (E_i) + \sum_i E_i\, Y_i\; SAF(E_i)} \qquad (3)$$

where the first term of the numerator is the contribution of beta emissions (if applicable) to the RBE weighted absorbed dose, the second term is the contribution of discrete electrons, and the third term is the contribution of photons (x- and gamma rays). The denominator is the unweighted absorbed dose. The mass of the tissue over which the dose is averaged is denoted by *M* and the energy and yield of the emitted radiations by *E* and *Y*, respectively. *SAF* denotes the fraction of the photon energy absorbed in the soft tissue of the body per unit mass (Eckerman *et al.* 2006), and RBE_E and RBE_P are the monoenergetic electron and photon RBE values of Tables 2 and 6, respectively.

The radionuclide-specific RBE values for 1070 radionuclides based on an energy cutoff of 5 keV are shown graphically in Fig. 9. For approximately 56% of the radionuclides the RBE values are less than 1.1. About 31% have RBEs between 1.1 and 1.3, and about 7% have RBEs between 1.5 and 2. Seventeen radionuclides are identified with an RBE of 2 or higher: ^{3}H (β^-, 12.32 y), ^{37}Ar (EC, 35.04 d), ^{41}Ca (EC, 1.02 x 10^5 y), ^{49}V (EC, 330 d), ^{53}Mn (EC, 3.7 x 10^6 y), ^{55}Fe (EC, 2.737 y), ^{59}Ni (EC β^+, 1.01 x 10^5 y), ^{68}Ge (EC, 270.95 d), ^{71}Ge (EC, 11.43 d), ^{123}Te (EC, 6.00 x 10^{14} y), ^{142m}Pr (IT, 14.6 m), ^{157}Tb (EC, 180 y), ^{163}Ho (EC, 4570 y), ^{187}Re (β^-, 4.12 x 10^{10} y), ^{193}Pt (EC, 50 y) , ^{194}Hg (EC, 440 y), and ^{205}Pb (EC, 1.53 x 10^7 y). The decay modes β^-, β^+, EC, and IT denote beta minus, beta plus, electron capture, and isomeric transition, respectively, and the units of the physical half-lives abbreviated m, d, and y are minute, day and year, respectively. The majority of the above nuclides decay by electron capture (EC), which is followed by a cascade of low energy Auger and Coster-Kronig electrons. Only three of the nuclides (^{3}H, ^{59}Ni, and ^{187}Re) are beta emitters (ICRP 2008); ^{59}Ni dominant mode of decay is by electron capture not by beta plus (positron) emission. The average energy of electrons emitted in the decay of ^{3}H, ^{59}Ni, and ^{187}Re is 5.7, 4.5, and 0.62 keV, respectively.

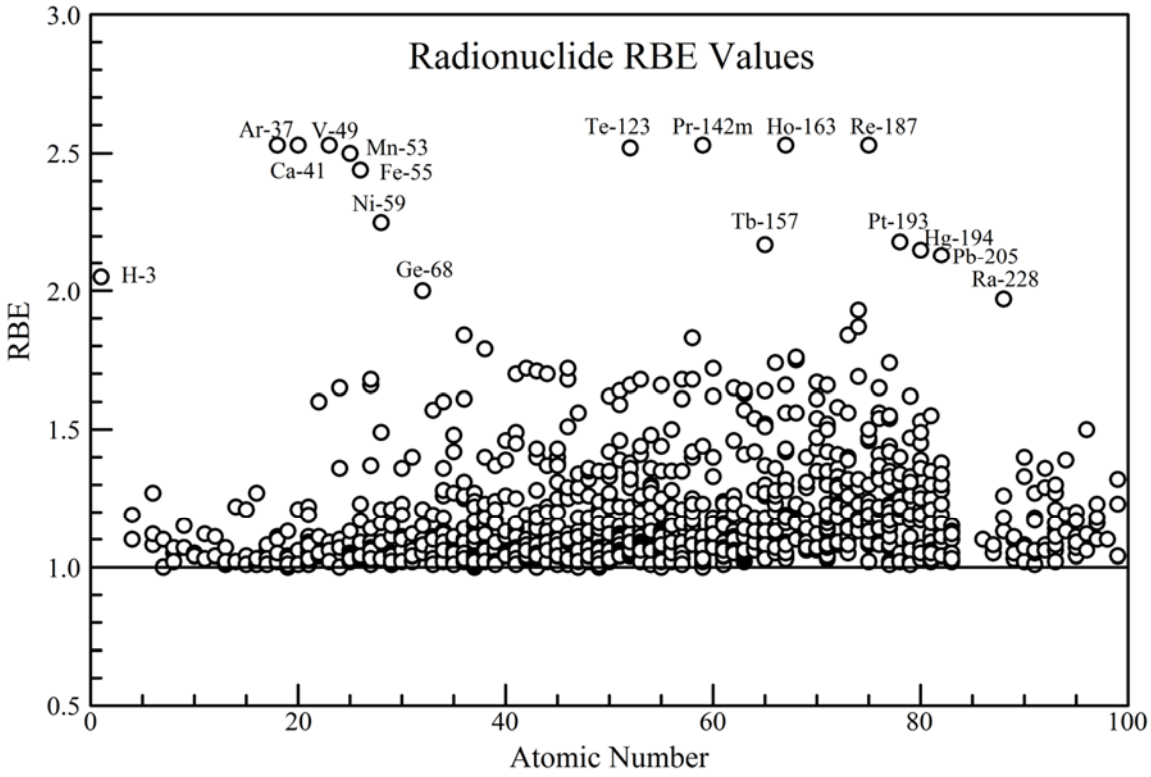

Fig. 9. Scatter plot of nuclide-specific RBE values. The reference radiation is 1 MeV electrons, and a 5 keV energy cutoff is assumed. The values were derived assuming the radionuclide is uniformly distributed in the soft tissues of the body. The majority of the radionuclides with RBE values above 2 decay by electron capture (EC), which is followed by a cascade of low energy Auger and Coster-Kronig electrons.

Table 2 Relative biological effectiveness of monoenergetic electrons relative to 1 MeV electrons based on various energy cutoff values, E_c.

Electron Energy (MeV)	E_c (keV)					
	1.5	**2.0**	**3.0**	**4.0**	**5.0**	**6.0**
0.0010	3.09	3.01	2.72	2.66	2.53	2.44
0.0015	3.09	3.01	2.72	2.66	2.53	2.44
0.002	2.59	3.01	2.72	2.66	2.53	2.44
0.003	2.10	2.30	2.72	2.66	2.53	2.44
0.004	1.88	2.02	2.31	2.66	2.53	2.44
0.005	1.75	1.85	2.07	2.30	2.53	2.44
0.006	1.67	1.74	1.91	2.09	2.29	2.44
0.008	1.57	1.62	1.73	1.85	1.97	2.11
0.010	1.50	1.54	1.63	1.71	1.81	1.90
0.015	1.41	1.43	1.48	1.53	1.58	1.64
0.02	1.36	1.38	1.41	1.44	1.48	1.52
0.03	1.30	1.31	1.32	1.34	1.37	1.38
0.04	1.28	1.28	1.29	1.30	1.32	1.33
0.05	1.24	1.25	1.26	1.27	1.28	1.29
0.06	1.22	1.23	1.24	1.25	1.25	1.26
0.08	1.20	1.20	1.20	1.21	1.21	1.21
0.1	1.17	1.17	1.18	1.18	1.19	1.19
0.15	1.16	1.16	1.16	1.16	1.16	1.15
0.2	1.12	1.12	1.12	1.12	1.12	1.13
0.3	1.10	1.11	1.11	1.11	1.11	1.11
0.4	1.06	1.07	1.07	1.07	1.07	1.07
0.5	1.03	1.03	1.03	1.03	1.03	1.03
0.6	1.01	1.01	1.01	1.01	1.01	1.01
0.8	1.00	1.00	1.00	1.00	1.00	1.00
1.0	1.00	1.00	1.00	1.00	1.00	1.00

Table 3. RBE values for selected beta emitting radionuclides relative to 1 MeV electrons.

	E_c (keV)					
Nuclide	**1.5**	**2.0**	**3.0**	**4.0**	**5.0**	**6.0**
H-3	1.67	1.74	1.86	1.97	2.05	2.11
C-14	1.23	1.24	1.24	1.26	1.27	1.28
P-32	1.01	1.01	1.01	1.01	1.01	1.01
Sr-90	1.11	1.11	1.11	1.11	1.12	1.12
Y-90	1.01	1.01	1.01	1.01	1.01	1.01

Table 4. Relative biological effectiveness of monoenergetic photons for various energy cutoff values E_c relative to 1 MeV electrons – full absorption.

Photon	E_c (keV)					
Energy (MeV)	**1.5**	**2**	**3**	**4**	**5**	**6**
0.010	1.50	1.55	1.63	1.71	1.81	1.90
0.015	1.42	1.44	1.49	1.53	1.58	1.63
0.020	1.38	1.40	1.43	1.46	1.50	1.53
0.030	1.36	1.38	1.41	1.42	1.44	1.46
0.040	1.39	1.41	1.45	1.47	1.49	1.50
0.050	1.41	1.43	1.48	1.52	1.55	1.57
0.060	1.40	1.43	1.48	1.52	1.55	1.68
0.08	1.41	1.44	1.49	1.53	1.57	1.60
0.10	1.40	1.42	1.47	1.51	1.55	1.68
0.15	1.36	1.38	1.42	1.45	1.48	1.51
0.20	1.32	1.34	1.37	1.39	1.42	1.44
0.30	1.27	1.28	1.30	1.31	1.33	1.35
0.40	1.23	1.24	1.25	1.27	1.28	1.29
0.50	1.20	1.21	1.22	1.23	1.24	1.25
0.60	1.17	1.18	1.19	1.20	1.21	1.21
0.80	1.12	1.13	1.13	1.14	1.15	1.15
1.0	1.09	1.09	1.10	1.10	1.11	1.11
1.17	1.08	1.08	1.08	1.09	1.09	1.10
1.33	1.07	1.07	1.07	1.08	1.08	1.09
1.5	1.06	1.06	1.06	1.07	1.07	1.08
2.0	1.04	1.04	1.05	1.05	1.05	1.06
3.0	1.03	1.03	1.03	1.03	1.03	1.04
4.0	1.02	1.02	1.02	1.02	1.02	1.02
5.0	1.02	1.02	1.02	1.02	1.02	1.02
6.0	1.01	1.01	1.01	1.01	1.01	1.01
8.0	1.01	1.01	1.01	1.01	1.01	1.01
10.0	1.01	1.01	1.01	1.01	1.01	1.01

Table 5. Relative biological effectiveness of monoenergetic photons for various energy cutoff values E_c relative to 1 MeV electrons – first interaction electrons.

Photon	E_c (keV)					
Energy (MeV)	1.5	2	3	4	5	6
0.010	1.50	1.55	1.63	1.71	1.81	1.90
0.015	1.42	1.44	1.49	1.53	1.58	1.63
0.020	1.38	1.40	1.43	1.46	1.50	1.53
0.030	1.36	1.38	1.41	1.42	1.44	1.46
0.040	1.40	1.42	1.46	1.50	1.54	1.54
0.050	1.42	1.45	1.50	1.54	1.58	1.61
0.060	1.44	1.47	1.52	1.57	1.58	1.65
0.08	1.43	1.45	1.50	1.54	1.58	1.62
0.10	1.38	1.40	1.44	1.47	1.51	1.54
0.15	1.30	1.32	1.34	1.36	1.38	1.40
0.20	1.25	1.25	1.26	1.28	1.29	1.30
0.30	1.19	1.20	1.20	1.21	1.21	1.21
0.40	1.15	1.15	1.15	1.16	1.16	1.16
0.50	1.13	1.14	1.14	1.14	1.14	1.15
0.60	1.10	1.11	1.11	1.11	1.11	1.12
0.80	1.06	1.06	1.07	1.07	1.07	1.07
1.0	1.04	1.04	1.04	1.04	1.05	1.05
1.17	1.03	1.03	1.03	1.03	1.04	1.04
1.33	1.02	1.02	1.02	1.02	1.03	1.03
1.5	1.02	1.02	1.02	1.02	1.02	1.02
2.0	1.01	1.01	1.01	1.01	1.01	1.01
3.0	1.01	1.01	1.01	1.01	1.01	1.01
4.0	1.00	1.00	1.00	1.00	1.00	1.00
5.0	1.00	1.00	1.00	1.00	1.00	1.00
6.0	1.00	1.00	1.00	1.00	1.00	1.00
8.0	1.00	1.00	1.00	1.00	1.00	1.00
10.0	1.00	1.00	1.00	1.00	1.00	1.00

Table 6. Recommended relative biological effectiveness for monoenergetic photons (5 keV energy cutoff values E_c) relative to 1 MeV electrons.

Photon Energy (MeV)	Photon RBE		
	Full Absorption	First Collision	Recommend
0.010	1.81	1.81	1.81
0.015	1.58	1.59	1.58
0.020	1.50	1.49	1.50
0.030	1.44	1.44	1.44
0.040	1.49	1.54	1.52
0.050	1.55	1.58	1.56
0.060	1.55	1.58	1.56
0.08	1.57	1.58	1.58
0.10	1.55	1.51	1.53
0.15	1.48	1.38	1.43
0.20	1.42	1.29	1.36
0.30	1.33	1.21	1.27
0.40	1.28	1.16	1.22
0.50	1.24	1.14	1.19
0.60	1.21	1.11	1.16
0.80	1.15	1.07	1.11
1.0	1.11	1.05	1.08
1.17	1.09	1.04	1.06
1.33	1.08	1.03	1.06
1.5	1.07	1.02	1.04
2.0	1.05	1.01	1.03
3.0	1.03	1.01	1.02
4.0	1.02	1.00	1.01
5.0	1.02	1.00	1.01
6.0	1.01	1.00	1.00
8.0	1.01	1.00	1.00
10.0	1.01	1.00	1.00

Table 7. Estimated RBE values relative to 1 MeV electrons for machine generated x-rays (tungsten anode) as a function of voltage and filtering.

X-ray source		Energy Cutoff (keV)					
Voltage (kVp)	**Filter (mm)**	**1.5**	**2**	**3**	**4**	**5**	**6**
20	1.2 Al	1.41	1.42	1.47	1.51	1.56	1.61
40	1.2 Al	1.37	1.39	1.42	1.44	1.47	1.50
80	1.2 Al	1.38	1.41	1.44	1.47	1.50	1.52
160	1.2 Al	1.39	1.41	1.45	1.49	1.52	1.54
250	1.2 Al	1.39	1.41	1.45	1.49	1.52	1.55
20	1.2 Al & 1 Cu	1.38	1.40	1.43	1.46	1.50	1.54
40	1.2 Al & 1 Cu	1.38	1.40	1.43	1.45	1.47	1.48
80	1.2 Al & 1 Cu	1.40	1.43	1.48	1.52	1.55	1.58
160	1.2 Al & 1 Cu	1.40	1.42	1.47	1.51	1.55	1.58
250	1.2 Al & 1 Cu	1.38	1.41	1.45	1.49	1.52	1.55

CONCLUSIONS

Results of experimental, computational and epidemiological studies indicate an increase in biological effectiveness of electron and photon radiations with decreasing energy of photons and electrons. The extent and shape of the increased RBE as a function of energy is difficult to determine with precision from the existing epidemiological and experimental studies. It appears that the increase in biological effectiveness is strongly associated with an increased density of ionization and excitation interactions, giving rise to an increase in clustered damage (multiply-damaged) sites in DNA. Monte Carlo simulations can be used to estimate frequencies of various categories of complex DNA damage produced, directly or indirectly, by the passage of ionizing radiation through tissue. However, due to a lack of detailed information on cellular processing of the DNA damage, it is not yet possible to predict from first principles the frequency or energy dependence of mutations – let alone cancers – induced by radiation.

Work carried out by Nikjoo and colleagues (Nikjoo *et al*. 1997, 2001, 2002) has shown that complex damage induction by passage of electrons through the cell nucleus is greatly enhanced near the ends of tracks, where the electron energy has been reduced to about 5 keV or lower. This suggests that the RBE for low-LET radiations may be strongly associated with the fraction of the dose deposited by electrons below 5 keV. This approach as implemented here led to an estimated RBE of about 2 for tritium beta particles relative to gamma rays of about 1 MeV or higher, in reasonable agreement with estimates derived from radiobiological data. As shown in Table 2, the estimate of RBE for electrons is relatively insensitive to the choice of cutoff energy.

Guided by the above considerations, we have estimated the RBEs for electrons and photons as a function of energy based on the fraction of energy deposited below certain cutoff energies. We adopted an energy cutoff of 5 keV which yielded a RBE for the tritium beta of 2, a rounded value consistent with suggestions by other expert groups who have addressed this issue. We then applied these results to obtain estimated RBEs for low-LET emissions by radionuclides of interest to EPA. Auger and Coster-Kronig electrons were not given special treatment, but if these emitters are indicated to be incorporated into the DNA then higher RBE values are warranted.

Uncertainties in the derived RBE are associated with uncertainties in:

- The empirical model
- Electron track codes
- Available electron cross-section data
- Water as a surrogate for tissue
- Assumed reference electron energy

The NOREC computer code used in this work has been shown to be in reasonable agreement with other electron track codes and representative of the current state-of-the-art (Nikjoo *et al*. 2006, Cho *et al.* 2007, Vassiliev 2012). Estimates of RBE for electrons and photons derived in this work were found to be fairly insensitive to the assumed electron cutoff energy and generally consistent with the available experimental data. The RBE values for machine generated x-rays were found to be less than 1.7 at all energies considered (20 to 250 kVp). Furthermore, no appreciable difference in RBE is indicated for 20 and 250 kVp x-rays. The RBE value for the ^{60}Co gamma rays of 1.06 (average of first collision value of 1.03

and full absorption value of 1.08 in Table 6) is slightly higher that the value of 1.01 derived for the photon fluence at a 1500 m ground distance from the hypocenter at Hiroshima and Nagasaki. The RBE value (1.01) derived here for the A-bomb spectra, based on the reference radiation being electrons of energy 1 MeV, is consistent with the assumed value of 1.0.

The dominant source of uncertainties in the derived RBEs would appear to arise from the employed empirical modeling approach which relates RBE to the fraction of absorbed dose deposited by low energy electrons. To provide further insight into the contribution of model uncertainty, an alternative modeling approach which simulates complex DNA damage might be undertaken. However the derived RBE values are noted to be consistent with those indicated by others although the values at low energy are somewhat less particularly for low-energy photons.

The RBE values derived here for electrons and photons are recommended for use in the revision of Federal Guidance Report 13. They should not be applied in a nuclide-specific manner as was done for the hypothetical analysis of Fig. 9. The recommended RBE values should be applied to the contribution to absorbed dose of emitted electron and photon radiations for the irradiated tissues associated with the various cancers addressed in the risk-expression models. In this manner the risk-expression of the particular cancer type will reflect the influence of age and gender on the absorbed dose contribution of these radiations.

References

Boudaiffa B, P Cloutier, D Hunting, M Huels, L Sanche (2000). Resonant formation of DNA strand breaks by low-energy (3 to 20 eV) electrons, *Science* **287**: 1658-1660.

Burch P (1957a). Calculation of energy dissipation characteristics in water for various radiations, aspects of relative biological efficiency, *Radiat Res* **6**: 289-301.

Burch P (1957b). Some aspects of relative biological efficiency, *Br J Radiol* **30:** 524-529.

Charlton DE, JL Humm (1988). A method of calculating initial DNA strand breakage following the decay of incorporated ^{125}I, *Int J Radiat Biol* **53:** 353-365.

Cho S, O Vassilev, J Horton (2007). Comparison between an event-by-event Monte Carlo code NOREC, and ETRAN for electron scaled point kernels between 20 keV and 1 MeV, *Radiat Environ Biophys* **47:** 77-83.

Dingfelder M, RH Ritchie, JE Turner, W Friedland, HG Paretzke and RN Hamm (2008). Comparisons of calculations with PARTRAC and NOREC: transport of electrons in liquid water, *Radiat Res* **169:** 584–94.

Dietze G and WG Alberts (2004). Why it is advisable to keep $w_R = 1$ and $Q = 1$ for photons and electrons, *Radiat Prot Dosim* **109**: 297-302.

Eckerman KF, RW Leggett, M Cristy, CB Nelson, JC Ryman, AL Sjoreen, RC Ward (2006). *User's Guide to the DCAL System*, ORNL/TM-2001/190, Oak Ridge National Laboratory, Oak Ridge, TN.

EPA (1994). *Estimating Radiogenic Cancer Risks, Addendum: Uncertainty Analysis*, EPA 402-R-93-076 (U.S. Environmental Protection Agency, Washington, DC).

EPA (1999a). *Cancer Risk Coefficients for Environmental Exposure to Radionuclides, Federal Guidance Report No. 13*, EPA 402-R-99-001 (Oak Ridge National Laboratory, Oak Ridge, TN; U.S. Environmental Protection Agency, Washington, DC).

EPA (1999b). Estimating Radiogenic Cancer Risks, EPA 402-R-93-076 (U.S. Environmental Protection Agency, Washington, DC).

EPA (2011). *EPA Radiogenic Cancer Risk Models and Projections for the U.S. Population*, EPA 402-R-11-001 (U.S. Environmental Protection Agency, Washington, DC).

Egbert S, G Kerr, H Cullings (2007). DS02 fluence spectra for neutrons and gamma rays at Hiroshima and Nagasaki with fluence-to-kerma coefficients and transmission factors for sample measurements, *Radiat Environ Biophys* **46:** 311–325.

Fabry L, A Wambersie (1985). Induction of chromosome aberration in Go human lymphocytes by low doses of ionizing radiations of different quality, *Radiat Res* **103**:122-134.

Frankenberg D, K Kelnhofer, K Bar, M Frankenberg-Schwager (2002a). Enhanced neoplastic transformation by mammography x-rays relative to 200 kVp x-rays. Indication for a strong dependence on photon energy of the RBE_M for various endpoints, *Radiat Res* **157**: 99-105. Erratum (2002) *Radiat Res* **158**:126.

Frankenberg D, K Kelnhofer, I Garg, K Bar, M Frankenberg-Schwager (2002b). Enhanced mutation and neoplastic transformation in human cells relative to 29 kVp relative to 200 kVp x-rays indicating a strong dependence of RBE on photon energy, *Radiat Prot Dosim* **99**: 261-264.

Frankenberg D, M Frankenberg-Schwager, I Garg, E Pralle, D Uthe, B Greve, E Severin, W Gohde (2002c). Mutation induction and neoplastic transformation in human and human-hamster hybrid cells: dependence on photon energy and modulation in the low-dose range, *J Radiol Prot* **22**: A17-20.

Folkard M, KM Prise, B Vojnovic, S Davies, MJ Roper and B D Michael (1993). Measurement of DNA damage by electrons with energies between 25 and 4000 eV, *Int J Radiat Biol* **64**: 651-658.

Friedland W, H Paretzke, F Ballarini, A Ottolenghi, G Kreth, C Cremer (2008). First steps towards systems radiation biology studies concerned with DNA and chromosome structure within living cells, *Radiat Environ Biophys* **47:** 49-61.

Goggelmann W, C Jacobsen, W Panzer, L Walsh, H Roos, E Schmid (2003). Re-evaluation of the RBE of 29 kV x-rays (mammography x-rays) relative to 220 kV x-rays using neoplastic transformation of human CGL1-hybrid cells, *Radiat Environ Biophysics* **42**:175-182.

Goodhead DT, J Thacker, R Cox (1979). Effectiveness of 0.3 keV carbon ultrasoft x-rays for the inactivation and mutation of cultured mammalian cells, *Int. J Radiat Biol* **36:** 101–14.

Goodhead D, J Thacker, R Cox (1981). Is selective absorption of ultrasoft x-rays biologically important in mammalian cells?, *Phys Med Biol* **26:** 1115.

Goodhead DT and H Nikjoo (1990). Current status of ultrasoft X-rays and track-structure analysis as tools for testing and developing biophysical models of radiation action, *Radiat Prot Dosim* **31**: 343-350.

Goodhead D (2006). Energy Deposition Stochastic and Track Structure: What About The Target?, *Radiat Prot Dosim* **122**: 3-15.

Hill MA (2004). The variation in biological effectiveness of X-rays and gamma rays with energy, *Radiat Prot Dosim* **112**: 471–48.

HPA (UK Health Protection Agency) (2007). *Review of Risks from Tritium. Report of the Independent Advisory Group on Ionising Radiation.* Documents of the Health Protection Agency. Radiation, Chemical and Environmental Hazards. www.hpa.org.uk/webc/HPAwebFile/HPAweb_C/1197382221858.

ICRP (International Commission on Radiological Protection) (2004). Relative Biological Effectiveness (*RBE*), Quality Factor (*Q*), and radiation weighting factor (w_R), ICRP Publication 92. *Ann ICRP* **33**.

ICRP (2007). 2007 Recommendations of the International Commission on Radiological Protection. ICRP Publication 103, *Ann. ICRP* **37**(2-4).

ICRP (2008). Nuclear Decay Data for Dosimetric Calculations. ICRP Publication 107, *Ann ICRP* **38**.

Kocher DC, AI Apostoaci, FO Hoffman (2005). Radiation effectiveness factors for use in calculating probability of causation of radiogenic cancer, *Health Phys* **89**: 3-32.

Krumrey M, G Ulm, E Schmid (2004). Dicentric chromosomes in monolayers of human lymphocytes produced by monochromatized synchrotron radiation with photon energies from 1.83 keV to 17.4 keV, *Radiat Environ Biophys* **43**: 1–6.

Land C, E Gilbert, J Smith, FO Hoffman, I Apostoaei, B Thomas, DC Kocher (2003). Report of the NCI-CDC working group to revise the 1985 NIH radioepidemiological tables. National Cancer Institute, Bethesda MD.

Little MP, BE Lambert (2008). Systematic review of experimental studies on the relative biological effectiveness of tritium, *Radiat Environ Biophys* **47:** 71–93.

Michael BD, P O'Neill (2000). A Sting in the Tail of Electron Tracks, *Science* **287**: 1603-1604.

Moissenko V, R Hamm, W Prestwich (2001). Calculation of radiation-induced DNA damage from photons and tritium beta-particles, *Radiat Environ Biophys* **40**: 23–31.

NAS (National Academy of Science) (2006). *Health Risks from Exposure to Low Levels of Ionizing Radiation: BEIR VII Phase 2*. Washington, DC: The National Academies Press.

NIOSH (2002). NIOSH-Interactive RadioEpidemiological Prorgram (IREP) technical documentation; Final report. National Institute for Occupational Safety and Health. Available at: www.cdc.gov/niosh/ocas/pdfs/irep/irepfnl.pdg.

Nikjoo H, D Goodhead (1991). Track structure analysis illustrating the prominent role of low-energy electrons in radiobiological effects of low-let radiations, *Phys Med Biol* **36:** 229-238.

Nikjoo H, P O'Neil, WE Wilson, DT Goodhead (2001). Computational Approach for Determining the Spectrum of DNA Damage Induced by Ionizing Radiation, *Radiat Res* **156**: 577-583.

Nikjoo H, P O'Neill, DT Goodhead, M Terrissoll (1997). Computational modeling of low-energy electron-induced DNA damage by early physical and chemical events, *Int J Radiat Biol* **71:** 467-483.

Nikjoo H, CE Bolton, R Watanabe, M Terrisol, P O'Neill, DT Goodhead (2002). Modelling of DNA damage induced by energetic electrons (100 eV to 100 keV), *Radiat Prot Dosim* **99**: 77-80.

Nikjoo H, S Uehara, D Emfietzoglou, FA Cucinotta (2006). Track-structure codes in radiation research, *Radiat Meas* **41**: 1052-1074.

Nikjoo H, L Lindborg (2010). Topical review: RBE of low energy electrons and photons, *Phys Med Biol* **55:** R65–R10.

Paretzke HG (1988). *Simulation von Elektronenspuren im Energiebereich 0.01-10 keV*. In GSF-Bericht, pp. 24-88. Wasserdampf Gesellschaft fur Strahlen- und Umwelt Forschung, Munchen.

Pelowitz, DB (2008). *MCNPX User's Manual*, Version 2.6.0. LA-CP-07-1473. Los Alamos National Laboratory, Los Alamos, NM.

Poludniowski G, G Landry, F DeBlois, PM Evans, F Verhaegen (2009). SpekCalc: a program to calculate photon spectra from tungsten anode x-ray tubes, *Phys Med Biol* **54**: N433-N438.

Roos, H, E Schmid (1998). Analysis of chromosome aberrations in human peripheral lymphocytes induced by 5.4 keV x-rays, *Radiat Environ Biophys* **36(4)**:251-254.

Semenenko V, JE Turner and T Borak (2003). NOREC, a Monte Carlo code for simulating electron tracks in liquid water, *Radiat Environ Biophys,* **42**: 213-217.

Straume T (1995). High-energy gamma rays in Hiroshima and Nagasaki: Implications for risk and w_R, *Health Phys* **69**: 954-956.

Turner JE, RN Hamm, ML Souleyrette, DE Martz, TA Rhea, DW Schmidt (1988). Calculations for beta dosimetry using Monte Carlo code (OREC) for electron transport in water, *Health Phys* **55**: 741–750.

Vassiliev ON (2012). Electron slowing-down spectra in water for electron and photon sources calculated with the Geant4-DNA code, *Phys Med Biol* **57**: 1087-1094.